Applied Geochemistry 137 (2022) 105201

Contents lists available at ScienceDirect

Applied Geochemistry

journal homepage: www.elsevier.com/locate/apgeochem

Refining the conceptual model for radionuclide mobility in groundwater in the vicinity of a Hungarian granitic complex using geochemical modeling

Petra Baják [a,*], Katalin Csondor [a], Daniele Pedretti [b], Muhammad Muniruzzaman [c], Heinz Surbeck [a], Bálint Izsák [d], Márta Vargha [d], Ákos Horváth [e], Tamás Pándics [d], Anita Erőss [a]

[a] *József and Erzsébet Tóth Endowed Hydrogeology Chair, Department of Geology, Institute of Geography and Earth Sciences, Faculty of Science, Eötvös Loránd University, Pázmány Péter sétány 1/c, 1117, Budapest, Hungary*

[b] *Dipartimento di Scienze della Terra "A. Desio", Università degli Studi di Milano, Via Mangiagalli 34, 20133, Milan, Italy*

[c] *Water Management Solutions, Geological Survey of Finland, Vuorimiehentie 5, 02151, Espoo, Finland*

[d] *Public Health Directorate, National Public Health Institute, Albert Flórián út 2-6, 1097, Budapest, Hungary*

[e] *Department of Atomic Physics, Institute of Physics, Eötvös Loránd University, Pázmány Péter sétány 1/a, 1117, Budapest, Hungary*

ARTICLE INFO

Editorial handling by Prof. M. Kersten

Keywords:
Groundwater
Drinking water
Uranium
PHREEQC
Redox changes

ABSTRACT

Groundwater is an important freshwater resource, which can be affected by geogenic radionuclide contamination. To make decisions regarding the use and management of groundwater, understanding the controls of radionuclide mobility is critical. In the southern foreland of a granitic outcrop in Hungary, high gross alpha activity concentration was measured in drinking water wells, related probably to the presence of uranium. It has been suggested that understanding of the groundwater flow system may be a key aspect to understand uranium mobility in groundwater. The goal of the present work was to elucidate the conceptual model of radionuclide mobility in the study area, focusing in particular on the geochemical controls of uranium. For this purpose, water samples were collected and nuclide-specific measurements for ^{226}Ra and radon isotopes were carried out, in addition to ^{234}U+^{238}U measurements, to increase the range of radionuclides and better understand their mobility. A geochemical modeling analysis involving redox-controlling kinetic reactions and a surface complexation model was developed to support the conceptual model. The results from the sampling indicate that excess of ^{234}U+^{238}U (3–753 mBq L^{-1}) contribute to the natural radioactivity measured in drinking water to a large degree. ^{226}Ra was measured in relatively low activity concentrations (<5–63 mBq L^{-1}) with the exception of three specific wells. Notable radon activity concentration was measured in the springwaters from Velence Hills (1.01–3.14 × 10^{5} mBq L^{-1}) and in interrelation with the highest (285–695 mBq L^{-1}) ^{226}Ra activity concentrations. The geochemical model suggests that uranium distribution is sensitive to redox changes in the aquifer. Its mobility in groundwater depends on the residence time of groundwater compared to the reaction time controlling the consumption of oxidizing species. The longer the flow path from the recharge point to an observation point where U is measured, the more likely it is that reducing conditions will be found in the aquifer and the elemental concentration U will be low.

1. Introduction

Groundwater is one of the most important freshwater resources on Earth. In certain countries, the excess of natural radionuclides in groundwater is a key issue that has attracted scientific attention (Stackelberg et al., 2018; Sherif and Sturchio, 2018). As the ingested radionuclides undergo radioactive decay, the emitted particles can damage cells and tissues in the human body. The risk from ionising radiation must be kept as low as possible, to this end strict regulations are in force regarding the radionuclide content of drinking water. The natural radionuclide content of groundwater is primarily determined by the geological background, particularly by the occurrence of felsic igneous rocks (e.g. granites and pegmatites), which usually contain high amounts of uranium and other radionuclides and which are found all over the world (Banning and Benfer, 2017).

The effective dose received from drinking water consumption (not including bottled mineral water consumption) largely arises from the presence of dissolved ^{400}K, ^{234}U, ^{235}U, ^{238}U, ^{226}Ra, ^{222}Rn and ^{228}Ra

* Corresponding author.
E-mail address: bajakpetra@student.elte.hu (P. Baják).

https://doi.org/10.1016/j.apgeochem.2022.105201
Received 14 June 2021; Received in revised form 4 January 2022; Accepted 6 January 2022
Available online 10 January 2022

(Beyermann et al., 2010; Vesterbacka et al., 2006). ^{210}Po and ^{210}Pb also contribute but to a lesser extent (Ahmed et al., 2018; Jia and Torri, 2007; Kinahan et al., 2020). In case of bottled mineral waters, the sources of internal exposure are mainly ^{228}Ra, ^{226}Ra and ^{210}Pb (Chmielewska et al., 2020; Pérez-Moreno et al., 2020).

Beside tritium and radon activity, gross alpha and gross beta activity measurements are used as preliminary screening methods to assess the risk of radioactive elements in drinking water. In the European Union, the recommended screening levels are 1.0×10^5 mBq L^{-1} for tritium, and 1.0×10^5 mBq L^{-1} for radon, 100 mBq L^{-1} for gross alpha activity concentration, and 1000 mBq L^{-1} for gross beta activity concentration, in order to keep the indicative dose lower than 0.1 mSv yr^{-1} (Council Directive, 2013/51/Euratom). If either the gross alpha activity concentration or the gross beta activity concentration exceeds the relevant threshold, analysis of specific radionuclides shall be required. In order to evaluate if the indicative dose received from the intake of radionuclides is a health concern, derived concentrations of the most common natural radionuclides were calculated. The derived concentration values of the radionuclides concerned in this paper are the following: 3000 mBq L^{-1} for ^{238}U, 2800 mBq L^{-1} for ^{234}U and 500 mBq L^{-1} for ^{226}Ra.

Beside drinking water quality issues, the natural radionuclide content of groundwater has also been studied for scientific purposes. The isotopes of uranium, radium, and radon have long been used as natural tracers in the study of groundwater flow systems (Eisenlohr and Surbeck, 1995; Erőss et al., 2012; Gainon et al., 2007; Gainon, 2008; Swarzenski, 2007). While the behavior of these radionuclides in rock-water systems has been investigated in depth (Bourdon et al., 2003; Osmond et al., 1983; Porcelli and Swarzenski, 2003; Rama and Moore, 1984; Sheppard, 1980), this knowledge has not yet been properly introduced to the competent authorities of drinking water supply.

Although the presence of radionuclides in groundwater is primarily determined by the presence of their source rocks (e.g. granites, rhyolites, phosphorites, black shales), the spatial distribution of elevated radionuclide activity concentration in aquifers is also controlled by solute transport occurring along the hierarchically organized groundwater flow paths. A combination of multiple physical and geochemical factors (from different hydraulic conductivities to different temperature, pH, redox potential, specific electric conductivity, ion compositions) can change geochemical conditions along the flow paths (Tóth, 1999, 2009). Hydrogeological research can help to understand the monitoring results of the groundwater derived drinking water regarding radioactivity (Bird et al., 2020; Csondor et al., 2020; Erőss et al., 2018; Szabo et al., 2012). Erőss et al. (2018) investigated the occurrence of ^{234}U+^{238}U (hereinafter referred to as uranium) activity concentrations in groundwater in the southern foreland of the Velence Hills, a granitic outcrop in Hungary, where gross alpha values above 100 mBq L^{-1} were measured in the waterworks' wells. Uranium activity concentration measurements of 30 samples were carried out and the results were evaluated using pressure-elevation profiles referring to the hydraulic properties of the groundwater flow system. Uranium activity concentration up to 753 mBq L^{-1} was explained by a conceptual model of the groundwater dynamics in the study area, which included the predominance of recharge areas characterized by oxidizing environments as key determinants for U mobility in the aquifers. Erőss et al. (2018) concluded that a better understanding of the groundwater flow systems can provide key information regarding the evolution and distribution of radionuclides in aquifers. Beside the geological factors, Erőss et al. (2018) suggested that the groundwater dynamics and associated geochemical environment should be taken into account for an informed use and management of groundwater resources in the presence of geogenic radionuclide contamination. However, Erőss et al. (2018) did not analyze other radionuclides, nor performed modeling analysis to quantitatively interpret their results in the context of the hydrogeological behavior of the study area such as supported by a geochemical modeling analysis.

The aim of this study was to refine the conceptual model presented by Erőss et al. (2018) through a more detailed analysis of nuclide-specific activity concentrations in groundwater in the same Hungarian area and through model-based analysis. Compared to the previous work, the study area was expanded to include the granitic complex of the Velence Hills and its whole foreland, in order to evaluate the geographical extension of the previously identified high radionuclide content of the groundwater. The new study involved 26 new sampling locations, including springs of the granitic outcrop of the Velence Hills and new boreholes which were not sampled before. Uranium, ^{226}Ra and radon isotopes were measured in every sample. Moreover, ^{226}Ra and radon activity concentrations were also determined in the samples taken in previous sampling campaigns. To complete the previously applied hydrogeological approach based on pressure-elevation profiles, the physico-chemical properties and the hydrogeochemical characteristics of the water samples were further evaluated.

Finally, a process-based geochemical modeling analysis was performed using PHREEQC software (Parkhurst and Appelo, 2013) to quantitatively validate the conceptual model and the governing hypothesis explaining the behavior of radionuclides in groundwater. Geochemical modeling has been widely adopted to elucidate the interpretation of processes in a variety of applications, which includes redox-sensitive mobility of contaminants in aquifers (e.g. Dalla Libera et al., 2020; Greskowiak et al., 2015; Ma et al., 2014). As groundwater is the exclusive source of drinking water in the study area, the process-based understanding of groundwater quality has a crucial role in water supply and resource management.

2. Material and methods

2.1. Study area

The study area is located in the southern foreland of Lake Velence (Hungary), as formerly delineated by Erőss et al., (2018) (Fig. 1). Northwest from the lake, in its catchment area outcrop the igneous rocks of the Velence Hills. The western part of the hills is constituted by a biotitic granite batholith. It is characterized by higher uranium (up to 9.9 ppm) and thorium (up to 48.2 ppm) concentration (Bérczi, 1982) than the crust average (in Vinogradov, 1962 3.5 and 18 ppm, respectively). The central and eastern parts of the hills are built up by metamorphosed andesite and intrusive quartzite with less significant uranium and thorium content (up to 2.24 ppm and 11.4 ppm, respectively). In the foreland of the lake, the crystalline basement is covered by an up to 400 m thick siliciclastic sequence deposited in lacustrine to fluvial environment (Mezősi, 2015). These deposits host the Pannonian aquifer and the Quaternary aquifer, which are the main groundwater reservoirs and serve as drinking water sources of the local settlements.

The Pannonian sequence starts with locally sourced conglomerate, sand, and gravelly sand deposited on the crystalline basement or on previously redeposited granitic material in lacustrine depositional setting (Gyalog and Ódor, 1983; Sztanó et al., 2016; Budai et al., 2019). The particle size can reach 10–20 cm and decreases away from the bedrock (Gyalog and Ódor, 1983). It is followed by finer grained deltaic and fluvial deposits. The deltaic sequence is composed of 2–10 m thick deltaic bodies forming coarsening upward sequences from muddy prodelta to sandy delta front deposits capped by heterolith delta top deposits (Sztanó et al., 2013; Magyar et al., 2019). The fluvial depositional system, feeding the deltas is built up by sandy fluvial channels and grey to variegated siltstones and sand-mud heterolithics deposited on the alluvial-plain (Gyalog and Horváth, 2004; Haas, 2012). Charred plant remains and lignite layers are typical in these successions (Sztanó et al., 2013). Opposed to the lacustrine sediments, these deposits were fed by a more distal source. Their mineralogical composition is dominated by quartz. Other minerals such as feldspar, muscovite, rock fragments, altered minerals, clay minerals are present in a decreasing frequency. Among heavy minerals, chlorite, garnet, epidote, magnetite and amphibolite are the most abundant (Juhász and Thamó-Bozsó, 2006;

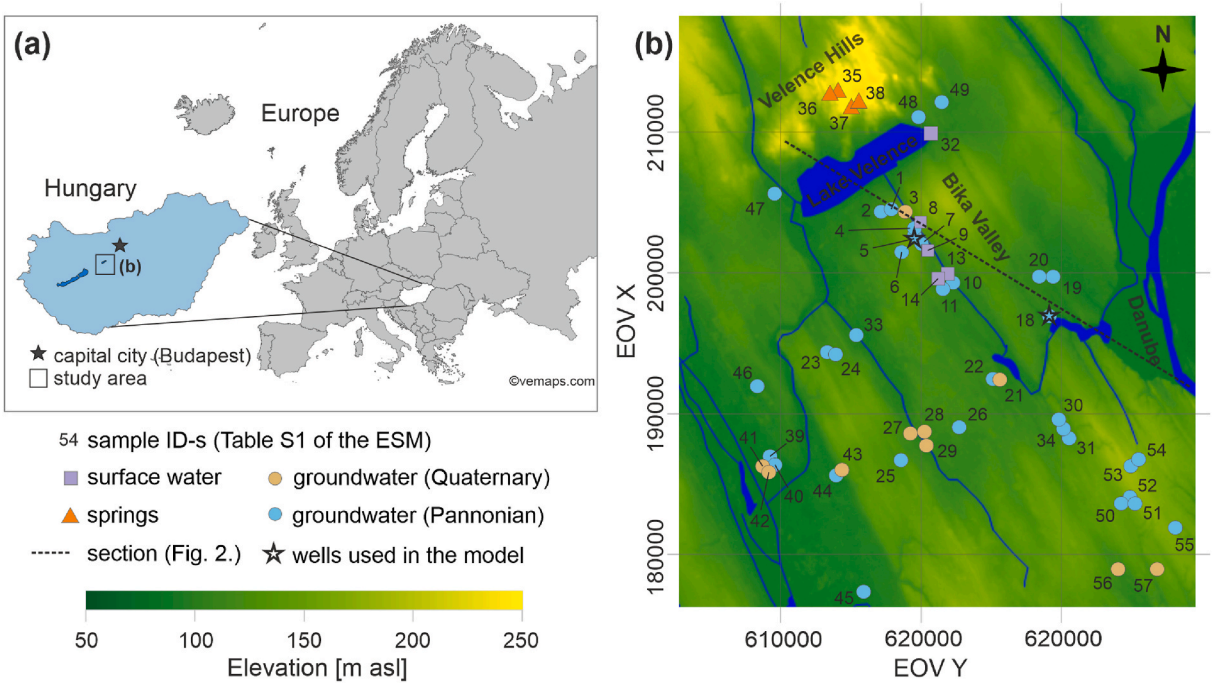

Fig. 1. a) Location of the study area. b) Sampling locations.

Thamó-Bozsó, 2002). The exploration for fissile materials established that the average uranium concentrations of the Pannonian formations are between 2.9 and 12.4 ppm. Although higher values are connected to the coaly-clayey beds (up to 290 ppm) and the carbonate cemented zones of sand and sandstone layers (up to 90 ppm) (Szilágyi and Glöckner, 1971).

The older formations are overlaid by a few meters thick siliciclastic Quaternary cover with a few outcrop exceptions, such as the Velence Hills. The Quaternary cover is made up of sediments of different origin (i.e. fluvial, lacustrine, eolic, eluvial, deluvial, proluvial) (Gyalog and Horváth, 2004). Loess is the most widespread formation with an average thickness of 2–5 m. In the proximity of the granitic area, it frequently contains fine grains of granite derived clasts. Loess mixed with eolic sand (sandy loess, loessy sand) covers the areas south of the Lake Velence. Besides the previous, redeposited clay and sand, derived from Pannonian sediments from eluvial and deluvial origin are frequent along the lake. Streams running from Velence Hills deposited sand and gravel. The youngest sediments are clayey–aleuritic formations filling the valleys, depressions and streambeds and peaty silt, calcareous clayey silt formed in the Lake Velence itself (Ádám, 1955). In general, the Quaternary sediments are characterized by higher quartz content than the Pannonian formations but have the same heavy mineral composition (e.g. chlorite, epidote, garnet) (Thamó-Bozsó, 2002).

2.2. Sampling

The present study added 26 new sampling locations to the 27 previously sampled sites as documented in the previous work by Erőss et al. (2018) (Fig. 1b). In total, 53 water samples were collected from 7 sampling campaigns carried out during 2018–2019. The samplings occurred in July and August 2018 (07/17, 08/16, 08/22 and 08/27) and in April 2019 (04/01, 04/02 and 04/18). The samples were taken from groundwater (N = 44), from surface water bodies (N = 5) and from springs (N = 4). The groundwater samples were collected from drilled wells screened into either the Pannonian sandstone (N = 34) or the Quaternary sand aquifer (N = 10). The wells are all continuously operating water supply wells owned by waterworks, companies or individuals. The elevation of the screened interval or measuring points for the collected water samples were from 96 m above sea level (asl) to −172 m asl. The sampled surface water courses are lakes and ponds situated in the research area with an elevation range of 107–141 m asl. The springs are located in the Velence Hills between 180 and 264 m asl and emanate from the granitic bedrock. The previously published dataset by Erőss et al., (2018) was also used during data processing to complement the interpretation of the results. The complete list of data used in this work is included as Table S1 of the electronic supplementary material (ESM).

The physicochemical properties of the water, such as specific electrical conductivity (±0.5%), temperature (±0.2 °C), pH (±0.2), Oxidation Reduction Potential (ORP, hereafter) (±20 mV), dissolved O_2 (±2%) were recorded on-site during the sampling by a YSI Pro Plus multiparameter water quality instrument (Xylem, USA). The accuracy of the device for each parameter is shown in parentheses. Water samples for elemental analysis were collected in 1.5 L PET bottles, 50 mL PP centrifuge tubes and 0.25 L glass bottles. For uranium and ^{226}Ra measurements, water samples were taken in 0.25 L polypropylene bottles. To determine radon activity concentration, liquid scintillation detection was used which requires specific sampling. On the previous day, 10 mL organic cocktail (Opti-Fluor O) was added into glass cuvettes, into which 10 mL water sample was injected by a syringe on-site and then the cuvettes were sealed by Parafilm M tape. All collected samples were kept cool at 5–10 °C until delivery to the laboratories.

2.3. Laboratory measurements

The hydrochemical analysis of the water samples was performed in the laboratories of the National Public Health Centre of Hungary and Eötvös Loránd University. The concentration of the major ions (Na^+, K^+, Ca^{2+}, Mg^{2+}, HCO_3^-, SO_4^{2-}, Cl^-, NO_3^-) and the trace elements (As, B, Ba, Be, Co, Fe, Li, Mn, Sr, Ti, V) were measured by ICP-MS (iCAP RQ, Thermo Fisher Scientific, Germany), ion chromatography (DIONEX ICS-5000 þ DP, Thermo Fisher Scientific, USA) and UV-VIS spectrophotometry (UV-1800, Shimadzu, Japan) in accordance with the relevant standard methods for drinking water (Standard MSZ EN ISO/IEC 17025:2005).

Uranium, ^{226}Ra and radon activity concentration measurements

were carried out from the collected water samples. Uranium was measured both by ICP-MS (after acidification by nitric acid) and with alpha spectrometry using NucFilm discs. For ^{226}Ra activity concentration measurements, only alpha spectrometry using NucFilm discs was applied (see Appendix S1 of the ESM, for further details on this measurement method). NucFilm discs are coated by selectively adsorbing thin films. The U-discs are made of polycarbonate, which is covered with epoxy resin fixing a finely ground ion exchange resin (Diphonix) that adsorbs actinides very selectively. Ra-discs are polyamide discs stained with MnO_2. In contact with water it works as a highly selective cation exchanger for heavy alkaline-earth ions. Some precautions are necessary, Ra-discs can be applied as long as the pH is above 4 and the barium concentration below 0.5 mg L^{-1} in the water sample (Surbeck 1996, 2000). All of our water samples meet these two requirements (Table S1 of ESM).

For ^{226}Ra and uranium measurements by NucFilm discs, 100 mL water sample is needed. As the first step, 20 mg EDTA (i.e. ethylenediaminetetraacetic acid) is added to the water to avoid carbonate precipitation. A Ra-disc is inserted and the sample is stirred for 8 h for an adsorption efficiency >90%. After the pre-treatment process, the disc is dried. Finally, the activity concentration of the ^{226}Ra adsorbed on the disc is measured by solid-state alpha detector with the measurement time of 24 h. The expected detection limit using 100 mL sample for one-day measurement is approximately 5 mBq L^{-1}. By using Ra-discs, ^{226}Ra activity concentration can be determined. As the pre-treatment is completed for ^{226}Ra measurement, the same water sample is acidified to pH 2–3 with concentrated (85%) formic acid. This treatment guarantees that uranyl-carbonate complexes are broken up. The U-discs are exposed to 100 mL acidified, stirred water for 20 h. After 20 h, 90% of the uranium activity present in the sample is adsorbed. The dried disc is subsequently measured with the alpha detector for another 24 h. Detection limit is the same as for ^{226}Ra (5 mBq L^{-1}). The calibration uncertainty of alpha spectrometry is ±20% compared to international standards. The alpha detector that is available in our laboratory measures the U-discs at ambient pressure. This is not only easier than in vacuum but also avoids contaminations of the detector by recoiled decay products. Thus, this method gives the sum of ^{234}U, ^{235}U and ^{238}U activity concentrations. Isotopic speciation was not considered in this study. As the ^{235}U activity contributes only about 5% of the ^{238}U activity, we use the term "uranium activity" to refer to the sum of the uranium isotopes (^{234}U+^{238}U).

The ICP-MS measurements determines mainly the ^{238}U elemental concentrations. Indeed, ^{234}U can be hardly detected by standard ICP-MS, given that ^{234}U has significantly lower abundance than ^{238}U. Since ICP-MS only provides ^{238}U elemental concentrations but alpha spectrometry includes both ^{234}U and ^{238}U, it is obvious that these two methods do not measure the same quantities and the correlation is not always 1:1. In this study, uranium elemental concentration [μg L^{-1}] measured by ICP-MS was only used as an input parameter during the geochemical modeling, whilst the activity concentration values [mBq L^{-1}] determined by alpha spectrometry were compared with the derived concentrations (laid down in Council Directive, 2013/51/Euratom) to assess the possible health effect. Radon activity concentration was measured with liquid scintillation detection using TriCarb 1000 TR in the laboratory within 2 days. The minimum detectable activity concentration of the TriCarb 1000 TR instrument is 2 × 10^3 mBq L^{-1}.

2.4. Geochemical modeling

The widely used geochemical code PHREEQC (Parkhurst and Appelo, 2013) was utilized for the quantification of key reactive processes controlling the speciation and mobility of radionuclides in the aquifer. Specifically, the analysis targeted the redox sensitivity of two main processes attenuating U, sorption-related processes and precipitation of U-bearing minerals. As this is the first study involving geochemical modeling in the area, the modeling only focused on the understanding of uranium mobility in groundwater, because the occurrence of Ra and Rn are local and lesser significant in this given area and the processes controlling their mobility are less well characterized than for U, therefore potentially complicating the interpretation of the model results.

The model is conceptualized as a batch-like kinetic reactor, which reproduces a transition from an oxic to an anoxic environment. The PHREEQC script to run the simulation can be accessed as Appendix S2 of the electronic supplementary material (ESM). The geochemical calculations including aqueous speciation, redox equilibria and mineral reactions were performed using the thermodynamic database *wateq4f* (Ball and Nordstrom, 1991). Although *wateq4f* already contains uranium complexes, the adopted database (attached as Appendix S3 of the ESM) was amended with the uranium complexes obtained from the more updated THEREDA database (Altmaier et al., 2011; Moog et al., 2015). Moreover, the dissolved ternary Ca-uranyl-triscarbonato complexes $CaUO_2(CO_3)_3^{2-}$ and $Ca_2UO_2(CO_3)_3$ by Maia et al. (2021) were also included in the thermodynamic database, considering that such complexes may also exert a control on uranium transport (e.g. Kersten 2021). The fact that we have included the new complexes in the database implicitly means that we were modeling the competition between the dissolved Ca uranyl carbonato complex formation and adsorption of uranyl carbonato complexes. Relevant model parameters, including the composition of the initial solution and other parameters involved in the modeling analysis, are listed in Table 1. As the key goal of the model was to provide a general understanding of processes controlling U mobility in the whole aquifer, the initial water composition was based on the average composition of oxidized waters enriched with U and sampled during the sampling campaigns. Specifically, we considered a composition similar to well nr. 4, which shows oxidizing water conditions (ORP = 124.9 mV) with a uranium elemental concentration of 1.3 × 10^{-2} mg kg^{-1} water. Total Fe concentration (missing for well nr. 4, due to problems with the measuring device) was assumed to be similar to the one collected at well nr. 48, i.e. Fe = 0.111 mg kg^{-1} water, which shows a comparable ORP condition.

The PHREEQC model is conceptually inspired by Fig. 2, with the following simple rationale: the longer the infiltrating water stays in a flow tube, the more prone that water is to undergo reducing conditions. Assuming homogeneous flow and geochemical conditions, the redox conditions along a flow tube from the recharge point to a discharge point change depending on the residence time of water T (s) compared to the time taken by soil reactions to generate a reducing environment. Using the Darcy's law, T can be computed as

$$T = \frac{L\theta}{Ki} \quad (1)$$

Table 1
Composition of the initial solution, kinetic and surface parameters used for the geochemical model.

Initial solution composition[a]		Kinetic and surface parameters	
pH	7.87	Initial organic matter [mol L^{-1}]	10
pe	4	k [s^{-1}]	1.0 × 10^{-14}
As	5.0 × 10^{-4}	Y_{O2} [mol L^{-1}]	2.94 × 10^{-4}
B	2.3 × 10^{-2}	Y_{NO3} [mol L^{-1}]	1.55 × 10^{-4}
Ba	0.116	Y_{SO4} [mol L^{-1}]	1.00 × 10^{-4}
C	494		
Ca	53	Initial surface sites	
Cl	10	Weak binding sites [mol L^{-1}]	1
Fe	0.111	Strong binding sites [mol L^{-1}]	1
K	2		
Li	3.1 × 10^{-2}		
Mg	44		
N(5)	10		
S	10		
Sr	1.2		
Ti	2.5 × 10^{-3}		
U	1.3 × 10^{-2}		
V	1.1 × 10^{-3}		

[a] The concentrations are in mg kg^{-1}w.

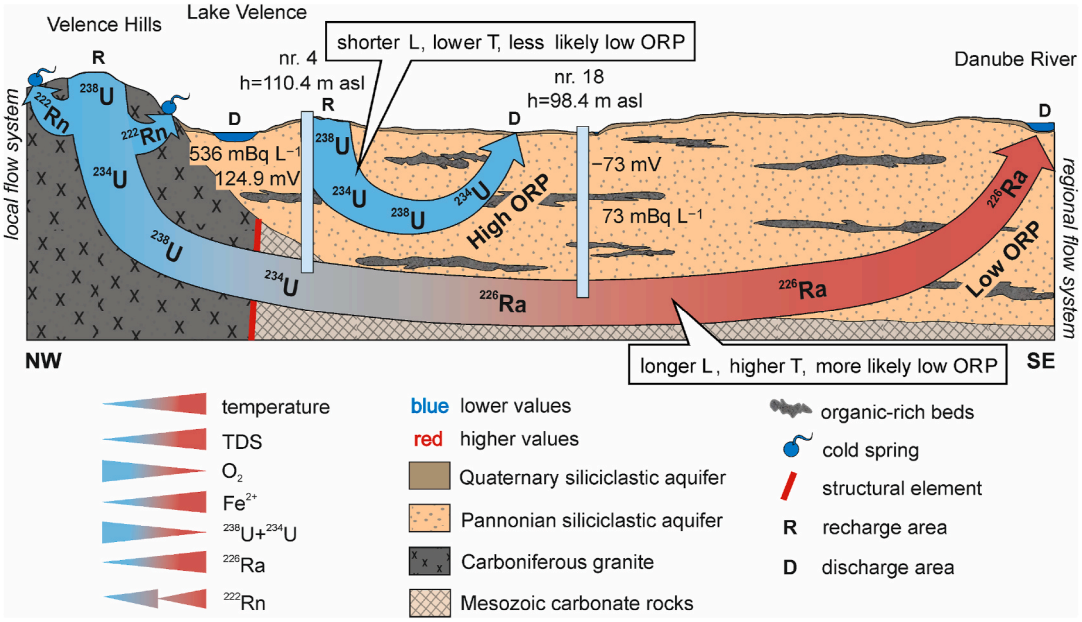

Fig. 2. Conceptual model explaining the relationship between length of the flow tube (L), residence time in the flow tube (T), which are related to the likelihood to create a reduced (low ORP) environment. Hydraulic head, ORP and uranium activity concentration values are shown for wells used for geochemical modeling. (Not to scale.)

where L is the travel length (m) between two points of the flow tube, θ is the porosity (−), K is the average hydraulic conductivity (ms^{-1}) along the flow tube and i is the hydraulic gradient (−), calculated from the groundwater head difference and the distance between two points of the flow tube. The longer the flow route L, the longer is the residence time T, and in turn the more likely that a flow tube will eventually experience reducing conditions at some distance from the infiltrating point. Such simplified model formulation is justified to identify mainly the key geochemical processes controlling the overall geochemistry in the aquifer, whereas a detailed multidimensional reactive transport model is required to capture the detailed dynamics of redox and radionuclides propagation fronts in the domain.

Given the organic-matter-rich (OM-rich) nature of the Pannonian aquifer, where the majority of the sampling was performed, we assumed kinetic OM degradation as the main driver of the redox change along a flow tube. The OM degradation can be described via additive Monod kinetic laws with multiple electron acceptors (eAs) (e.g. Appelo and Postma, 2005 p.526). Here, we utilized three eAs, namely O_2, NO_3^-, and SO_4^{2-}, such that the relative change in OM concentrations (C_{OM}) with time can be written as

$$\partial C_{OM} \Big/ \partial t = r_{OM} = -kC_{OM}\left(\frac{[O2]}{Y_{O2}+[O2]}+\frac{[NO3-]}{Y_{NO3-}+[NO3-]}+\frac{[SO42-]}{Y_{SO42-}+[SO42-]}\right) \quad (2)$$

where r_{OM} (mol L^{-1} s^{-1}) is the overall reaction rate, k is the first-order maximum degradation rate (s^{-1}), and Y_X is the half-saturation constant of the "X" EA (mol L^{-1}).

Under oxidizing conditions, U(VI) can sorb on a generic surface. Sorption of U was modelled using a surface complexation model (SCM), which assumed hydrous ferric oxide (Hfo) as the main phase containing two different types of the sorption sites (i.e. "strong" and "weak" sites, Dzombak and Morel, 1990). We adopted the simplest form of the surface complexation model without explicit treatment of diffuse double-layer (DDL) and/or Stern layer mechanisms (Appelo and Postma, 2005 p.326). The corresponding thermodynamic calculations along with the surface reactions for the SCM are performed with the standard *wateq4f* database. For the uranyl carbonate species, we have included the surface reactions from Mahoney et al. (2009), which summarized the dataset obtained from different studies and corrected the thermodynamic parameters for the old Dzombak and Morel (1990) model.

As the system tends to reducing conditions, U(VI) becomes U(IV). Under these conditions, uraninite [UO_2] and other minerals may precipitate. Uraninite is the simplest mineral, readily found in many environments in the world and is the predominant U mineral to precipitate in this system over a range of pH and at low to extremely low Eh (Cumberland et al., 2016). As such, uraninite was used in the model as the main sink of U in mineral phases. Despite the dominating siliciclastic nature of the aquifers, carbonate minerals are dispersed in the studied domain, contributing to buffer the groundwater acidity. Therefore, calcite was included as the main pH-buffering mineral. Surface complexation, uraninite precipitation and calcite dissolution are usually fast reactions, they were modelled as equilibrium reactions.

3. Results

3.1. Hydrochemistry

The 34 groundwater samples taken from the Pannonian aquifer represent the 96 to −172 m asl elevation interval according to the elevation of the screened sections of the wells (Fig. 3a, b). Most of the samples are characterized by low mineralization (609–827 μS cm^{-1}) based on the field recorded electrical conductivity (EC) values (Table S2 of the ESM). The EC values show no clear correlation with the screened-

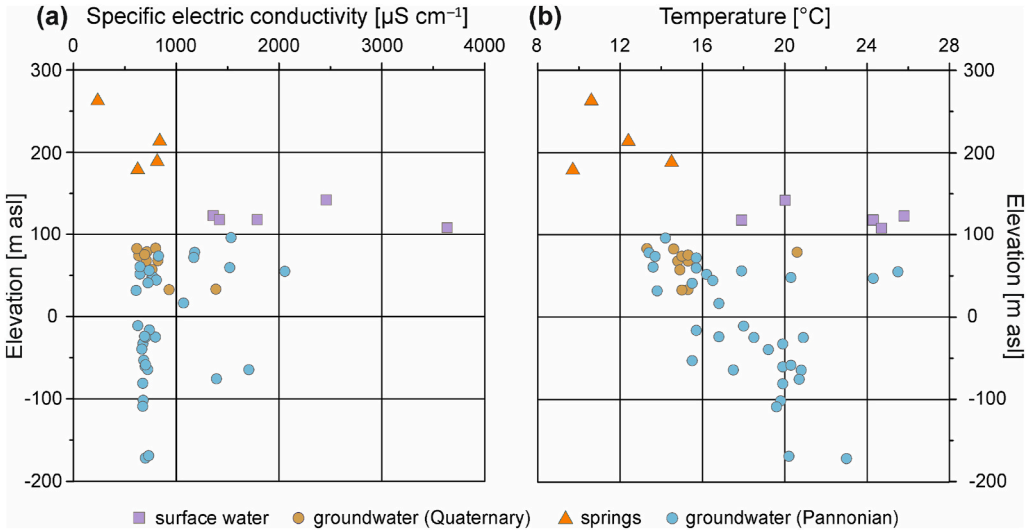

Fig. 3. a) The variation of electrical conductivity of the wells versus elevation profile. b) Temperature versus elevation profile of the sampled wells.

interval depth.

Eight Pannonian groundwater samples (nr. 2, 7, 23, 24, 25, 40, 48) have higher (1070–2056 µS cm^{-1}) EC values. Samples nr. 2, 7, 23, 24, 25 and 48 were taken from shallow wells (up to 77 m depth). Their high concentration of either Na^{+}, SO_4^{2-} or NO_3^{-} most likely had anthropogenic causes (i.e. agricultural activity, sewage effluent). Although sample nr. 6 was collected from a well that has higher depth (196 m), that specific well belongs to a farm. In the case of samples nr. 40 and 44, the cause is possibly natural (NO3- lower than 0.5, Na–K–HCO3- facies). The 10 water samples taken from the Quaternary aquifer represent a narrower screened elevation range of 33–83 m asl (Fig. 3a,b). The range of EC (616–930 µS cm^{-1}) characterizing the Quaternary aquifer is consistent with the range of values characterizing the Pannonian aquifer (Table S2 of the ESM). The sample nr. 41 shows the highest EC value (1385 µS cm^{-1}), which is also having one of the highest sulfate concentrations (140 mg L^{-1}). It is likely that sample nr. 41 is directly affected by anthropogenic activity, thus not being representative of natural aquifer conditions. All sampled groundwaters have circumneutral pH, consistent with the presence of pH-buffering carbonate minerals of the siliciclastic aquifers' cement. The pH of the Pannonian samples is generally higher (up to 8.13) than that of the Quaternary samples (up to 7.53) (Fig. 4). Quaternary samples have a narrower range

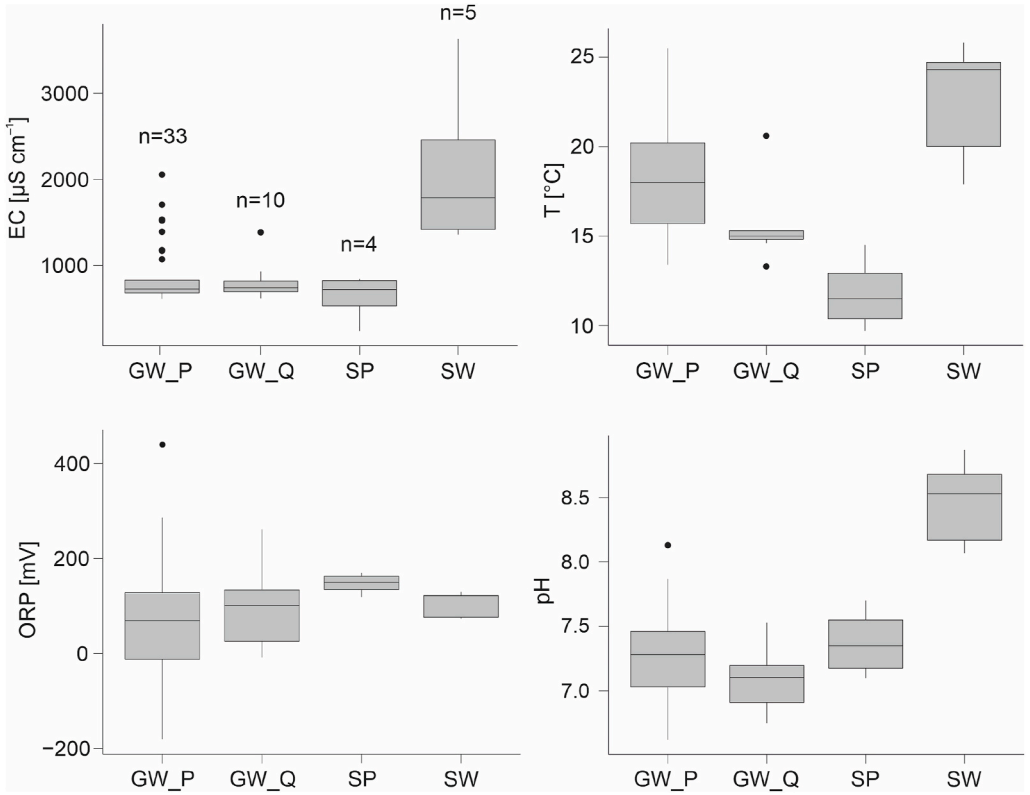

Fig. 4. The variation of the physico-chemical parameters. Samples with different origins are distinguished (GW_P: samples from the Pannonian aquifer; GW_Q: samples from the Quaternary aquifer; SP: spring waters; SW: surface waters).

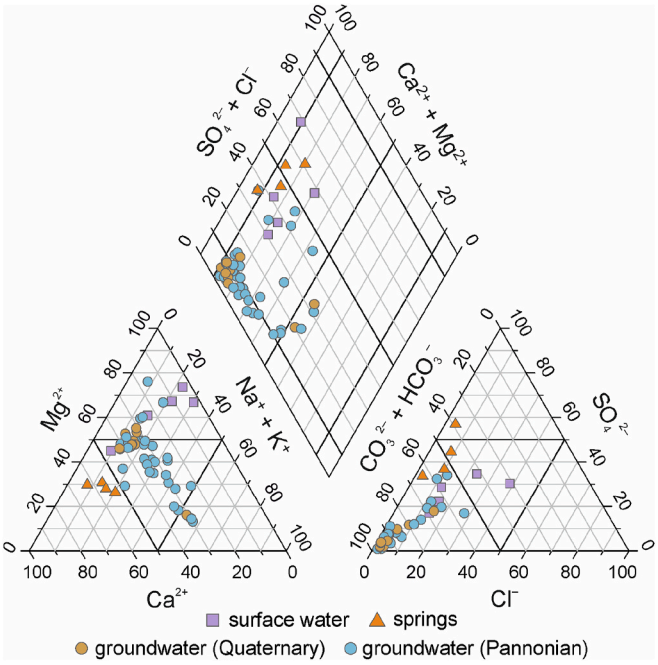

Fig. 5. Piper-diagram shows the results of water chemistry analysis of the water samples. Hydrochemical facies and the dominant anions, cations can be determined.

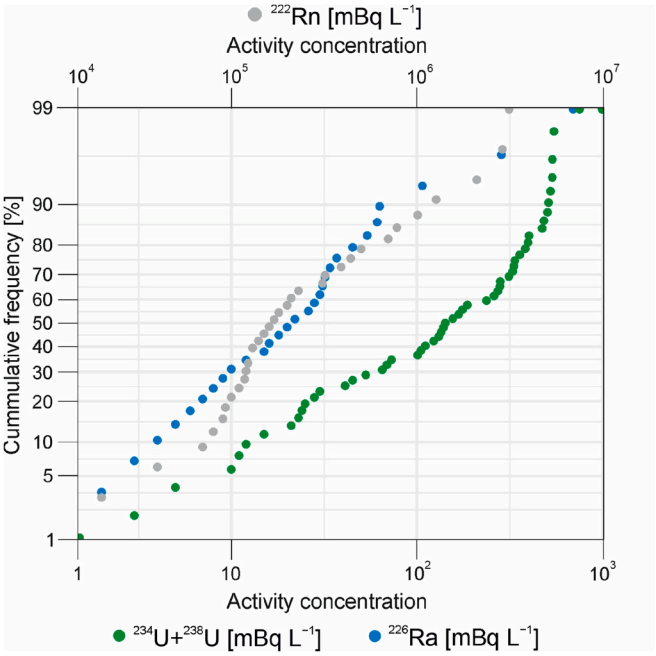

Fig. 6. Cumulative frequencies of the measured radionuclides ($^{234}U+^{238}U$, ^{226}Ra and ^{222}Rn) showing a lognormal distribution.

of temperature (13.3–15.3 °C) with an outlier (20.6 °C in nr. 3), whilst Pannonian samples have more variable temperature values between 13.4 and 25.5 °C (Fig. 4). According to the ORP measurements, oxidizing conditions are predominant among the collected samples. Two of the Quaternary samples (range: 9–261 mV) and eleven of the Pannonian samples (range: 181–440 mV) represent reducing conditions with their negative ORP values (Fig. 4).

The most prevalent anion in all groundwater samples is HCO_3^-, while there is no dominant cation (Fig. 5). Among the Quaternary samples, 5 of them have a dominant cation: in samples nr. 3, 22 and 57 magnesium is dominant; in nr. 41 and 42 sodium and potassium are dominant. On the other hand, 2 of the Pannonian samples have sodium-potassium as the prevalent cations and 3 of them are characterized by magnesium dominance. The most common hydrochemical facies (40 of the 44 samples) identified from Piper-plot is the calcium-magnesium-bicarbonate facies.

The five surface water samples (lakes) have both higher EC (range: 1359–3635 μS cm^{-1}) and pH (8.07–8.87) values compared to groundwater (Table S2 of the ESM). These samples have relatively high temperature among the water samples (17.9–25.8 °C) (Fig. 3b). Their dominant ions are HCO_3^- and Mg^{2+} as well, in one case there is neither a dominant cation or an anion (Fig. 4). Springs in the Velence Hills have the lowest EC (236 μS cm^{-1}) and temperature (9.7 °C) value (Table S2 of the ESM) of the sampled waters. Unlike groundwater samples, springs have calcium as the dominant cation and either HCO_3^- or SO_4^{2-} as the dominant anion (Fig. 5). Both surface water and spring samples represent oxidizing conditions (73–170 mV).

3.2. Radiochemistry

Among the measured radionuclides, uranium were measured in the highest activity concentration in all sample types (Fig. 6). All activity concentration values are at least an order of magnitude lower than the derived concentrations of ^{238}U and ^{234}U (3000 and 2800 mBq L^{-1}, respectively) in the drinking water quality recommendation. In groundwater samples the activity concentrations vary between 3 and 753 mBq L^{-1}, though Quaternary samples show lower activity concentrations (up to 524 mBq L^{-1}) than Pannonian samples (up to 753 mBq L^{-1}) (Table S3 of the ESM). Most of the highest uranium activity concentration values occur in the 100–0 m asl elevation interval (mean = 513.6 mBq L^{-1}; with a maximum of 753 mBq L^{-1}), while under 0 m asl lower (mean = 30.83 mBq L^{-1}) values were measured with a few exceptions (nr. 6, 10, 30, 31, 54; mean = 241.8 mBq L^{-1}). These exceptional samples were all taken from recharge areas (according to the research done by Erőss et al., 2018), where groundwater flows downwards, so that the oxidizing environment can be generated in greater depth compared to discharge areas. In surface water samples collected from 107 to 141 m asl elevation, uranium activity concentrations were

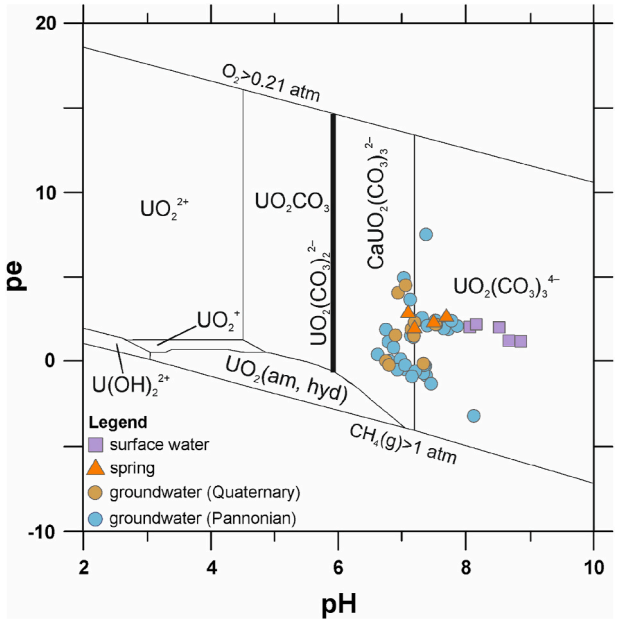

Fig. 7. Pourbaix diagram for uranium based on the thermodynamic database published by Mühr-Ebert et al. (2019) showing dominant species of uranium in complexing aqueous medium.

measured with an average of 346 mBq L^{-1} (Table S3 of the ESM). Springs emerging from the granitic bedrock present on the highest elevation of 180–264 m asl with an average uranium activity concentration of 153.25 mBq L^{-1}. Examining the spatial distribution of the elevated uranium activity concentrations, several groups can be distinguished with different locations e.g. Velence Hills, Bika Valley, local settlements. It can be concluded that the highest uranium values are not restricted to an easily delineated specific area. Samples collected from the so-called Bika Valley running from SE towards the Lake Velence are characterized by highest uranium activity concentration values.

The Pourbaix diagram can be generated for the sampled waters based on the ORP and pH values measured on site. It shows the stability of the various U-complexes (Fig. 7). The samples are in the negatively charged carbonate complex stability field of $UO_2(CO_3)_3^{4-}$ and $CaUO_2(CO_3)_3^{2-}$.

For ^{226}Ra, most of the samples are characterized by very low activity concentration (<5–63 mBq L^{-1}). ^{226}Ra activity concentration higher than the derived concentration of 500 mBq L^{-1} was measured in a Pannonian groundwater sample (nr. 23). Relatively high ^{226}Ra activity concentrations (107 and 285 mBq L^{-1}) were determined in two other Pannonian groundwater samples (nr. 18 and 46, respectively). The well nr. 18 has one of the deepest screened elevation intervals (−169 m asl) and its ORP referred to reducing conditions (−73.5 mV). The wells nr. 23 and nr. 46 are sampling a much shallower elevation interval (72 and 74 m asl, respectively) and ORP measurements are showing oxidizing conditions (85 and 69 mV, respectively). In the latter two wells, relatively high uranium activity concentrations (537 and 168 mBq L^{-1}, respectively) were determined in addition to the ^{226}Ra activity, suggesting that the interpretation of radium controlling processes may be complicated in the study area. These two sampled wells are located relatively close to each other (ca. 6 km away) on the left side of the study area, whilst the well nr. 18 is on the opposite side of the area alongside a small lake close to the Danube.

No radon activity concentration was measured in the surface water samples. This was anticipated considering that radon leaves the hydrosphere rapidly to the atmosphere via volatilization. Up to 3.14×10^5 mBq L^{-1} radon activity concentration was determined in the samples collected from the springs of the Hills. Most of the Pannonian groundwater samples have very low radon activity concentration (<0.5–7.8×10^4 mBq L^{-1}) with two notable exceptions exceeding the 1×10^5 mBq L^{-1} limit in wells nr. 23 and nr. 46 (2.89 and 1.27×10^5 mBq L^{-1}, respectively), corresponding to the previously presented high ^{226}Ra activity concentrations. In groundwater samples collected from the Quaternary aquifer the activity concentrations are even lower (0.8–7.0×10^4 mBq L^{-1}). The highest radon activity concentrations are concentrated in the Hills and on the left side of the area interrelated with the high ^{226}Ra activity concentrations measured in that location.

3.3. Model results

Fig. 8 and Fig. 9 show the main results of the modeling analysis. In all plots, the horizontal axis represents the time of the simulation in years. In Fig. 8, panel a) shows the elemental concentrations of dissolved uranium as U(VI) and U(IV), computed by the PHREEQC. Ferric iron is also shown for comparison purposes. In panel b), the elemental concentrations of uranium (U(IV)) adsorbed on weak ("Hfo(w)") and strong ("Hfo(s)") sorptive surfaces are shown. In panel c), the redox potential (expressed as pe) and the saturation index (SI) of uraninite are shown.

As depicted in Fig. 8, the model suggests that for short time scales (corresponding to short residence time of water in a flow tube, or to a short flow path) the system remains under oxidizing conditions (pe above 0). Under these conditions, uranium is highly mobile, being present as U(VI). Uraninite appears to be undersaturated (SI < 0) and the sorption sites are occupied by an amount of uranium which is in equilibrium with the elemental concentration present in the aqueous phase. With time, the aqueous elemental concentrations of U(VI) tend to increase slightly (Fig. 8a), likely due to the slight decrease in pe, causing a

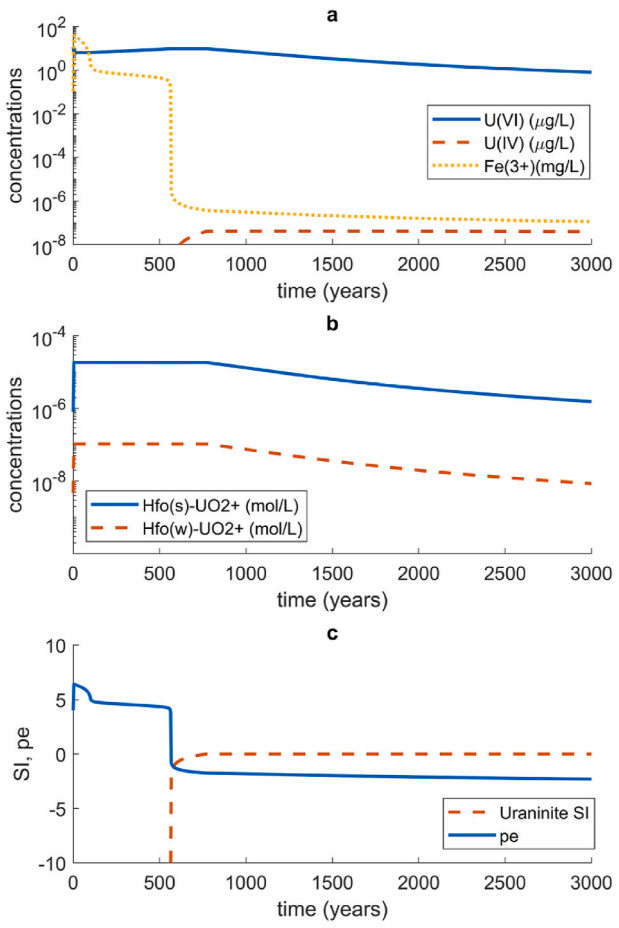

Fig. 8. Results from the PHREEQC analysis. a) Elemental concentrations of redox-sensitive species, U(IV), U(VI) and Fe^{3+}, showing a change in concentrations around 500 years with a decrease in U(IV) when reducing conditions prevail. b) Elemental concentration of uranium on weak and strong sorptive surfaces (hydroferric oxides, Hfos). c) Redox potential (expressed as pe) and saturation index (SI) of uraninite, rapidly tending to SI = 0 when reducing conditions occur.

shift in equilibrium with the Hfo surfaces and consequently a release of uranium from the surface to the pore-water (Fig. 8b). This is consistent with the field observation. In some cases, we observed that the total U content is higher at boreholes which are located downstream from others, and therefore away from the recharge zone. For example, samples (nr. 5, 4, 1) derived from the Pannonian aquifer within a screened elevation interval of 44–56 m asl in Bika Valley show an increasing uranium activity concentration toward Lake Velence (402, 536, 753 mBq L^{-1}, respectively). The same phenomenon has been observed elsewhere (e.g. Dhaoui et al., 2016).

Setting the rate coefficient used for the OM degradation kinetic law (Eq. (2)) to $k = 1.00 \times 10^{-14}\ s^{-1}$, the model suggests a sudden change in oxidizing-reducing potential occurring in the aquifer at t ≈ 560 years. This is reflected by a drop in the calculated pe, tending to pe = −2. Note that, in real life, the change in oxidizing-reducing potential could be less discontinuous, although such an effect cannot be reproduced by our model. A different model, such as based on an advection-dispersion-reaction model, may be used to replicate a more realistic smoother transition between high and low pe values. We devise the development of such a model as a future development of this study. The time at which the system transitions from high low to pe values agrees well with the mean residence time T of water flowing from wells nr. 4 (located in the Bika Valley running towards the lake from SE) to well nr. 18 (located on the right side of the study area alongside a small lake close to the

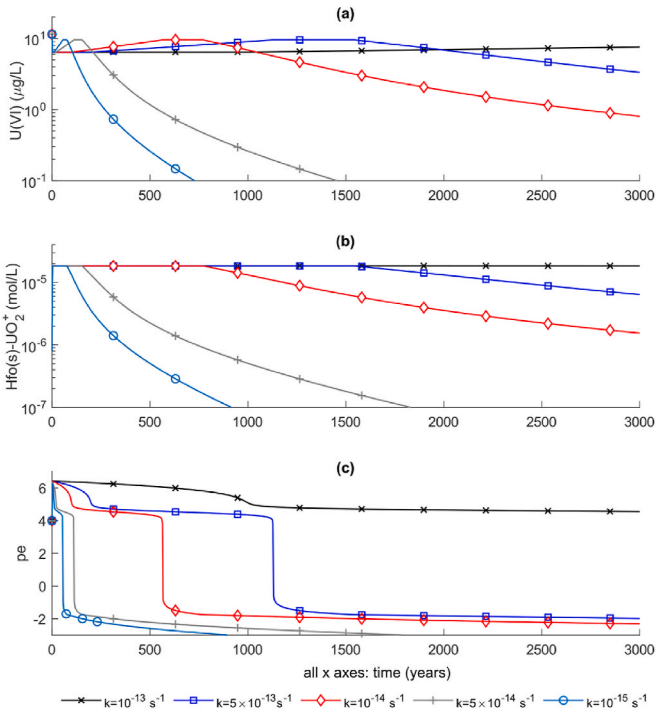

Fig. 9. Sensitivity analysis around the rate coefficient k used for the OM degradation kinetic law (Eq. (2)). The resulting (a) elemental concentrations of U(IV) as aqueous form and (b) bound to the strong Hfo surfaces and (c) the pe are compared.

Danube). The wells lie along the main regional groundwater direction towards the Danube River. From nr. 4 to nr. 18, we observed a transition from ORP = 90 mV to ORP = −73 mV, which corresponds to a pe from 5 to 6 to about 2 (considering the instrumentation error and the range of possible conversion factors from ORP to pe – e.g. Wolkersdorfer, 2008 p.183). Recalling Equation (1), we considered a porosity $\theta = 0.2$, a hydraulic conductivity $K = 5 \times 10^{-5}$ ms^{-1} (values representative of the bulk Pannonian aquifer, e.g. Mádl-Szőnyi and Tóth, 2009) and a hydraulic gradient $\underline{i} = 1.5 \times 10^{-3}$ calculated from the head difference Δh = 12 m between these points, which are separated by L ≈ 8×10^3 m. This results in a residence time T=676 years. While the minimum pe values observed during the new sampling campaign were limited to values of pe ≈ 0 (at well nr. 33, where ORP = −181 mv), it should be noted that the actual ORP values at the sampling points may be lower than the measured values. Indeed, we should recall the notorious difficulties to conduct reliable in-situ measurements of redox potential, as the groundwater tends to rapidly equilibrate with the oxidized atmosphere.

As the system tends to reducing conditions, U(VI) transforms to U(IV) while uraninite precipitates, becoming a sink of uranium. The groundwater chemistry adjusts to the new redox equilibrium by releasing uranium from the Hfo surfaces, which also contribute to the formation of uraninite. Consequently, the calculated U elemental concentrations drop from values close to a maximum of 34 μg L^{-1} to 0.09 μg L^{-1}, which agrees with the range of measured values (from 18 μg L^{-1} to 1.5 μg L^{-1}).

The rate k controlling the time scales of the transition from an oxidized to a reducing status was key for this modeling exercise. While the adopted values for the results shown in Fig. 8 are consistent with those reported in literature for nitrate and sulfate reduction (e.g. Appelo and Postma, 2005), the parameter k remains uncertain. A sensitivity analysis around the parameter k was therefore performed to study the implication of this parameter on the behavior of uranium and controlling variables. The results are shown in Fig. 9. It was found that the model is very sensitive to the adopted kinetic rate. A change of k towards higher values (i.e. quicker OM degradation) causes a faster depletion in EAs, and consequently U(IV) tends to attenuate more rapidly. On the contrary, a change of k towards lower values (i.e. slower OM degradation) causes a delay in the attenuation process, leaving U(VI) mobile for longer time scales. It is therefore concluded that a proper assessment of the kinetic rate k may be critical to make adequate model-supported decisions regarding the mobility of uranium in the studied aquifer.

4. Discussion

The results of this new study corroborate and further support the conceptual model proposed by Erőss et al. (2018), which suggested a direct control of groundwater dynamics on radionuclide mobility.

The groundwater tapping either the Pannonian or the Quaternary aquifers show very similar geochemical characteristics in the extended study area. The newly collected samples (nr. 32–57) have common features regarding their physical and chemical properties to those presented by Erőss et al., (2018) (nr. 1–31). This is due to the extensive Pannonian and Quaternary aquifers used widespreadly in the vicinity of Velence Hills. The relatively low temperature (17.5 °C on average) and EC (869 μS cm^{-1} on average) values and the positive ORP values (76 mV on average) measured in the groundwater samples seem to support the hydrogeological configuration described in Erőss et al., (2018). According to this configuration, the groundwater samples were collected from recharge areas and mainly local flow systems penetrating in shallow depth were sampled. Close to the River Danube, a well (nr. 18) with almost the deepest screened elevation (−169 m asl) may sample a regional flow limb moving from higher elevation (i.e. Vértes Mountains and Velence Hills) toward its discharge point (i.e. Danube River). These results correspond with the conceptual model presented by Gainon (2008) which indicates that high uranium activity concentrations occur along local flow limbs and in recharge areas where the geochemical environment modified by the groundwater is favorable for uranium dissolution and mobilization (i.e. oxidizing conditions exist).

The extended study area and the results of new samplings, with uranium activity concentration up to 358 mBq L^{-1}, confirmed that uranium contributes to the gross alpha activity concentration above the screening value to a large degree. The extension of the study area and the collection of more water samples revealed that the elevated uranium activity concentration is not limited only to the wells located in the southern foreland of Lake Velence. The drinking water supply wells used in other settlements in the wider area are also concerned. Consequently, it can be concluded that this is a widespread phenomenon in the studied area, i.e. several private and company owned wells deliver groundwater with elevated radioactivity due to uranium, which are out of the scope of the regulatory monitoring. However, no health concern arises from uranium consumption because the derived concentrations of ^{234}U and ^{238}U isotopes are relatively high (2800 and 3000 mBq L^{-1}, respectively) and all measured activity concentrations (up to 753 mBq L^{-1}) are generally an order of magnitude lower.

Relatively high ^{226}Ra (up to 695 mBq L^{-1}) and radon activity concentrations (up to 2.89×10^5 mBq L^{-1}) were also determined in specific wells (nr. 23, 46). The presence of ^{226}Ra may indicate that these wells sample the reducing water of a regional groundwater flow system. Given the 3.8 days long half-life of radon, its high activity concentration may suggest the existence of a local radon source, which is most likely iron and manganese oxyhydroxide precipitation (Erőss et al., 2012; Gainon et al., 2007; Kovács-Bodor et al., 2019). These wells belong to the local waterwork and the precipitations may be artificial (water distribution pipes or the water treatment chemicals can be the sources of the iron) beside natural causes (iron- and manganese-bearing minerals naturally occurring in the aquifer). Further investigations might be necessary to understand the phenomenon responsible for the ^{226}Ra and radon activity concentration exceeding the limit values (500 mBq L^{-1} and 1×10^5 mBq L^{-1}, respectively) and to estimate the health risk arising from the concurrence of these radionuclides in drinking water.

The Pourbaix diagram based on Mühr-Ebert et al. (2019) identifies the possible aqueous forms of uranium as $UO_2(CO_3)_3^{4-}$ and $CaUO_2(CO_3)_3^{2-}$. The Pannonian siliciclastic aquifers are mainly cemented by carbonate cement (Gyalog and Horváth, 2004). The hydrochemical analysis revealed that the prevalent anion in the analysed groundwater samples is HCO_3^- and the common hydrochemical facies is calcium-magnesium-bicarbonate. These hydrochemical properties can be related to the carbonate cement and enable the formation of the above-mentioned complexes. Moreover, Szilágyi and Glöckner (1971) mentioned a possible form of uranium accumulation as the repeating solution and precipitation of this cement. The granitic rocks of the Velence Hills with its relatively high thorium and uranium content (Bérczi, 1982) is a possible source rock and it is located upstream from the high uranium activity concentration values along the assumed regional flow system travelling from NW to SE. To reveal if the granite has an impact on the radionuclide content of the waters in the study area, the springs in Velence Hills were sampled. Based on the significant annual changes of the discharges of the springs and their low temperature (up to 14.5 °C) they are presumably the discharge points of local flow systems. The EC values (up to 842 μS cm^{-1}) are likely biased due to anthropogenic impact. Radon anomalies in the soil gas and in the springs in the Hills have been studied thoroughly (Minda et al., 2009; Torres et al., 2018) and the source of the radon was identified as monazite-group minerals and allanite (Burján et al., 2002). However, other radionuclides in the springwaters were measured only by this study and revealed elevated (up to 337 mBq L^{-1}) uranium content of springwaters beside radon (up to 3.14×10^5 mBq L^{-1}).

The results of the geochemical modeling with PHREEQC further support the conceptual model proposed by Erőss et al. (2018) and confirmed in the present study, by which uranium is mainly controlled by redox-sensitive processes. The modeling highlighted that the wide range of uranium activity concentration can be explained by complex rock-water interactions existing in recharge areas and along their paths towards the discharge points. The modeling exercise developed with PHREEQC illustrates well the capacity of geochemical models to support decisions when dealing with the excess of radionuclide in groundwater. Although simplified compared to a real-life complex geochemical system, the batch-like model results already provide quantitative information about some of the relevant processes that can control the occurrence of U and overall chemistry in groundwater. It should be however highlighted that the model presents some limitations.

The most critical limitation is that the aquifer is a multidimensional, physically and geochemically heterogeneous system in which multiple boundary conditions (such as lakes, springs, rainfall driven recharge or rivers) concur directly or indirectly in the control of the radionuclide dynamics. The geochemical system is more complicated than the one simulated in this work. The model presented here does not simulate transport explicitly. One consequence is that the sharp redox front reproduced in Figs. 8 and 9 is unlikely to occur in reality. Mechanisms such as mixing and spreading contribute to the smearing the redox front, as well as controlling the extension of geochemical reactions occurring in the aquifer (e.g. Dentz et al., 2011). Heterogeneity controls the time scaling of solute transport in the different parts of aquifers (Bianchi and Pedretti, 2018), with direct consequence on the ratio between transport and reaction time scales as well as on the geometry of the flow tubes.

Furthermore, electrostatic effects induced by the ionic and surface charge might exert additional controls on the reaction fronts (e.g., Appelo et al., 2008, 2010; Muniruzzaman et al., 2014; Muniruzzaman and Rolle, 2017; Rolle et al., 2013; Tournassat and Steefel, 2015). Such Coulombic effects and electrical double layer (EDL) mechanisms can be particularly relevant in the current system because of slow groundwater flow velocities (e.g. Boudreau et al., 2004; Giambalvo et al., 2002; Muniruzzaman and Rolle, 2015, 2019; Soler et al., 2019).

These limitations shall be addressed in a more detailed and dedicated future modeling analysis. All listed mechanisms can be included in a multidimensional reactive transport model (Steefel et al., 2015). Codes based on PHREEQC were successfully applied to reproduce multidimensional U transport at the Hanford site in the USA (Ma et al., 2010), and they could be deployed to reproduce U and other radionuclide transports in the present study area.

5. Conclusion

A new study was performed to evaluate the occurrence and controls of geogenic radionuclide mobility in groundwater in the southern foreland of the Velence Hills, a granitic outcrop in Hungary. The area was previously investigated by Erőss et al. (2018), who focused on uranium mobility and concluded that groundwater dynamics may have a direct impact on radionuclide mobility in the area.

The present work extended the former research done by Erőss et al. (2018) by adding (1) new sampling points, which included springs and boreholes never sampled before, (2) nuclide-specific measurements of the new sampled waters, namely of uranium, ^{226}Ra and radon, (3) measurements of ^{226}Ra and radon on samples taken from previous campaigns, and (4) geochemical modeling for a quantitative interpretation of the uranium controlling processes.

The main conclusions achieved from this work can be listed as follows:

- Groundwater derived from the extensive Pannonian and Quaternary aquifer share similar geochemical characteristics but present a wide range of activity concentrations of radionuclides among which uranium reaches the highest values.
- Besides aquifer lithology and flow dynamics, the local geochemical processes along the flow path have the major control on the range of uranium activity concentrations.
- Geochemical modeling is a crucial tool for understanding radionuclide mobility in complex aquifers. The model is able to quantify the effect of strongly nonlinear processes, such as the interplay between the kinetic degradation of organic matter (generating reducing conditions) and the attenuating mechanisms that remove uranium from the aqueous system. It was shown that a simple batch-like model is able to provide similar time scales for the transition from oxidizing to reducing conditions, which results in a change in uranium elemental concentration in groundwater from >10 μg L^{-1} to <1 μg L^{-1}.
- The monitoring strategy should include nuclide-specific measurements in case of gross activity concentrations exceeding the screening values, since only nuclide-specific measurements facilitate the complex understanding of the interrelationship of geological sources and transport processes of groundwater flow.
- The collection and analysis of more water samples pointed out that uranium contributes to the natural radioactivity of groundwater to the largest degree, but no health risk arises from its radiological properties because the measured activity concentrations are lower than the derived activity concentration of 2800–3000 mBq L^{-1}, specified in the relevant regulation. One well should be further investigated, where ^{226}Ra activity concentration above the 500 mBq L^{-1} derived concentration and radon exceeding the 1×10^5 mBq L^{-1} screening value was determined.

The results of this new study corroborate and further support the conceptual model proposed by Erőss et al. (2018), which suggested a direct control of groundwater dynamics on radionuclide mobility. Therefore, application of process-based geochemical modeling can support decision making when dealing with radionuclide excess in drinking water. Those areas can be delineated where the geochemical environment along with the hydrogeological properties are favorable for uranium mobilization by the groundwater and therefore more frequent quality monitoring may be crucial.

Declaration of competing interest

The authors declare that they have no known competing financial interests or personal relationships that could have appeared to influence the work reported in this paper.

Acknowledgements

This topic is part of a project that has received funding from the European Union's Horizon 2020 research and innovation programme under grant agreement No 810980. This study was also supported by the ÚNKP-17-4-III-ELTE-73 New National Excellence Program of the Ministry of Human Capacities (Hungary). The results here presented have been developed in the frame of the MIUR Project "Dipartimenti di Eccellenza 2017—Le Geoscienze per la società: risorse e loro evoluzione". Constructive reviewes by executive editor Michael Kersten, associate editor Gareth Law and the anonymous reviewers significantly improved the manuscript. The help of László Szikszay in the laboratory is greatly acknowledged. The contributions of Soma Budai are appreciated. Special thanks to those companies and private citizens, who enabled water sampling from their own wells.

Appendix A. Supplementary data

Supplementary data to this article can be found online at https://doi.org/10.1016/j.apgeochem.2022.105201.

References

Ádám, L., 1955. A Velencei-tó és a Zámolyi medence kialakulása. Foldtani Kozlony 79 (39), 307–332.
Ahmed, M.F., Alam, L., Mohamed, C.A.R., Mokhtar, M.B., Ta, G.C., 2018. Health risk of Polonium 210 ingestion via drinking water: an experience of Malaysia. Int. J. Environ. Res. Publ. Health 15 (10), 2056. https://doi.org/10.3390/ijerph15102056.
Altmaier, M., Bube, C., Marquardt, C., Brendler, V., Richter, A., Moog, H.C., Scharge, T., Voigt, W., Wilhelm, S., 2011. THEREDA Thermodynamic reference database. Summary of final report 66 (GRS – 265) ISBN 978-3-939355-41– 0). Germany.
Appelo, C.A.J., Postma, D., 2005. Geochemistry, Groundwater and Pollution. CRC Press, Boca Raton, p. 683. https://doi.org/10.1201/9781439833544.
Appelo, C.A.J., Vinsot, A., Mettler, S., Wechner, S., 2008. Obtaining the pore water composition of a clay rock by modeling the in- and out-diffusion of anions and cations from an in-situ experiment. J. Contam. Hydrol. 101 (1-4), 67–76. https://doi.org/10.1016/j.jconhyd.2008.07.009.
Appelo, C.A.J., Van Loon, L.R., Wersin, P., 2010. Multicomponent diffusion of a suite of tracers (HTO, Cl, Br, I, Na, Sr, Cs) in a single sample of Opalinus Clay. Geochem. Cosmochim. Acta 74, 1201–1219. https://doi.org/10.1016/j.gca.2009.11.013.
Ball, J.W., Nordstrom, D.K., 1991. User's Manual for Wateq4f, with Revised Thermodynamic Database and Test Cases for Calculating Speciation of Major, Trace, and Redox Elements in Natural Waters, vol. 90. USGS Open-File Report, p. 129. https://doi.org/10.3133/ofr90129.
Banning, A., Benfer, M., 2017. Drinking water uranium and potential health effects in the German Federal State of Bavaria. Int. J. Environ. Res. Publ. Health 14 (8), 927. https://doi.org/10.3390/ijerph14080927.
Bérczi, J., 1982. Velencei Hegységi Térképezés Során Gyűjtött Minták Neutronaktiválásos Vizsgálata És Értékelése. Budapesti Műszaki Egyetem. Kézirat. Országos Földtani és Geofizikai Adattár, Budapest.
Beyermann, M., Bünger, T., Schmidt, K., Obrikat, D., 2010. Occurrence of natural radioactivity in public water supplies in Germany: 238U, 234U, 235U, 228Ra, 226Ra, 222Rn, 210Pb, 210Po and gross α activity concentrations. Radiat. Protect. Dosim. 141 (1), 72–81. https://doi.org/10.1093/rpd/ncq139.
Bianchi, M., Pedretti, D., 2018. An entrogram-based approach to describe spatial heterogeneity with applications to solute transport in porous media. Water Resour. Res. 54 (7), 4432–4448. https://doi.org/10.1029/2018WR022827.
Bird, K.S., Navarre-Sitchler, A., Singha, K., 2020. Hydrogeological controls of arsenic and uranium dissolution into groundwater of the Pine Ridge Reservation, South Dakota. Appl. Geochem. 114, 104522 https://doi.org/10.1016/j.apgeochem.2020.104522.
Bourdon, B., Turner, S., Henderson, G.M., Lundstrom, C.C., 2003. Introduction to U-series geochemistry. Rev. Mineral. Geochem. 52, 1–21. https://doi.org/10.2113/0520001.
Boudreau, B.P., Meysman, F.J.R., Middelburg, J.J., 2004. Multicomponent ionic diffusion in porewaters: coulombic effects revisited. Earth Planet Sci. Lett. 222, 653–666. https://doi.org/10.1016/j.epsl.2004.02.034.
Budai, S., Sebe, K., Nagy, G., Magyar, I., Sztanó, O., 2019. Interplay of sediment supply and lake-level changes on the margin of an intrabasinal basement high in the Late Miocene Lake Pannon (Mecsek Mts., Hungary). Int. J. Earth Sci. 108 https://doi.org/10.1007/s00531-019-01745-3, 2001–2019.
Burján, Zs, Nagy-Balogh, J., Gál-Sólymos, K., Szabó, Cs, 2002. Spectrochemical study of potential source minerals of radon anomaly. Microchem. J. 73 (1–2), 47–51. https://doi.org/10.1016/S0026-265X(02)00049-8.
Chmielewska, I., Chałupnik, S., Wysocka, M., Smoliński, A., 2020. Radium measurements in bottled natural mineral-, spring-and medicinal waters from Poland. Water Resour. Industry 24, 100133. https://doi.org/10.1016/j.wri.2020.100133.
Council Directive 2013/51/EURATOM.
Csondor, K., Baják, P., Surbeck, H., Izsák, B., Horváth, Á., Vargha, M., Erőss, A., 2020. Transient nature of riverbank filtered drinking water supply systems-A new challenge of natural radioactivity assessment. J. Environ. Radioact. 211, 106072 https://doi.org/10.1016/j.jenvrad.2019.106072.
Cumberland, S.A., Douglas, G., Grice, K., Moreau, J.W., 2016. Uranium mobility in organic matter-rich sediments: a review of geological and geochemical processes. Earth Sci. Rev. 159, 160–185. https://doi.org/10.1016/j.earscirev.2016.05.010.
Dalla Libera, N., Pedretti, D., Tateo, F., Mason, L., Piccinini, L., Fabbri, P., 2020. Conceptual model of arsenic mobility in the shallow alluvial aquifers near Venice (Italy) elucidated through machine learning and geochemical modeling. Water Resour. Res. 56 (9), e2019WR026234 https://doi.org/10.1029/2019WR026234.
Dentz, M., Le Borgne, T., Englert, A., Bijeljic, B., 2011. Mixing, spreading and reaction in heterogeneous media: a brief review. J. Contam. Hydrol. 120, 1–17. https://doi.org/10.1016/j.jconhyd.2010.05.002.
Dhaoui, Z., Chkir, N., Zouari, K., Ammar, F.H., Agoune, A., 2016. Investigation of uranium geochemistry along groundwater flow path in the Continental Intercalaire aquifer (Southern Tunisia). J. Environ. Radioact. 157, 67–76. https://doi.org/10.1016/j.jenvrad.2016.03.00.
Dzombak, D.A., Morel, F.M.M., 1990. Surface Complexation Modelling- Hydrous Ferric Oxide. John Wiley, New York, p. 416.
Eisenlohr, L., Surbeck, H., 1995. Radon as a natural tracer to study transport processes in a karst system. An example in the Swiss Jura. Cr. Acad. Sci. II. A. 321 (9), 761–767.
Erőss, A., Mádl-Szőnyi, J., Surbeck, H., Horváth, Á., Goldscheider, N., Csoma, A.É., 2012. Radionuclides as natural tracers for the characterization of fluids in regional discharge areas, Buda Thermal Karst, Hungary. J. Hydrol. 426, 124–137. https://doi.org/10.1016/j.jhydrol.2012.01.031.
Erőss, A., Csondor, K., Izsák, B., Vargha, M., Horváth, Á., Pándics, T., 2018. Uranium in groundwater–The importance of hydraulic regime and groundwater flow system's understanding. J. Environ. Radioact. 195, 90–96. https://doi.org/10.1016/j.jenvrad.2018.10.002.
Gainon, F., Goldscheider, N., Surbeck, H., 2007. Conceptual model for the origin of high radon levels in spring waters–the example of the St. Placidus spring, Grisons, Swiss Alps. Swiss J. Geosci. 100 (2), 251–262. https://doi.org/10.1007/s00015-007-1220-6.
Gainon, F., 2008. Les isotopes radioactifs de la série de l'uranium-238 (222Rn, 226Ra, 234U et 238U) dans les eaux thermales de Suisse: sites d'Yverdon-les-Bains, Moiry, Loèche-les-Bains, Saxon, Val d"Illiez, Bad Ragaz, Delémont, Lavey-les-Bains, Brigerbad et Combioula. Thèse CHYN, p. 109.
Giambalvo, E.R., Steefel, C.I., Fisher, A.T., Rosenberg, N.D., Wheat, C.G., 2002. Effect of fluid-sediment reaction on hydrothermal fluxes of major elements, eastern flank of the Juan de Fuca Ridge. Geochem. Cosmochim. Acta 66, 1739–1757. https://doi.org/10.1016/S0016-7037(01)00878-X.
Gyalog, L., Ódor, L., 1983. Felső-Pannóniai bázisképződmények a Velencei-hegység keleti részén. In: Magyar Állami Földtani Intézet Évi Jelentése Az 1981 Évről, pp. 413–423.
Greskowiak, J., Gwo, J., Jacques, D., Yin, J., Mayer, K.U., 2015. A benchmark for multi-rate surface complexation and 1D dual-domain multi-component reactive transport of U(VI). Comput. Geosci. 19, 585–597. https://doi.org/10.1007/s10596-014-9457-4.
Gyalog, L., Horváth, I. (Eds.), 2004. Geology of the Velence Hills and the Balatonfő. Explanatory Book of the Geological Map of the Velence Hills (1:25 000) and the Geological Map of Pre-sarmatian Surface of the Balatonfő–Velence Area (1:100 000). Geological Institute of Hungary, Budapest.
Haas, J. (Ed.), 2012. Geology of Hungary, first ed. Springer-Verlag, Berlin Heidelberg.
Jia, G., Torri, G., 2007. Estimation of radiation doses to members of the public in Italy from intakes of some important naturally occurring radionuclides (238U, 234U, 235U, 226Ra, 228Ra, 224Ra and 210Po) in drinking water. Appl. Radiat. Isot. 65 (7), 849–857. https://doi.org/10.1016/j.apradiso.2007.01.022.
Juhász, Gy, Thamó-Bozsó, E., 2006. Az alföldi pannóniai s.l. képződmények ásványi összetétele II. - a pannóniai s.l. homokok és homokkövek ásványi összetétel változásának tendenciái és földtani jelentőségük. Foldtani Kozlony 136 (2), 431–450.
Kersten, M., 2021. Comment on "enthalpy of uranium adsorption onto hematite". Environ. Sci. Technol. 55 (5), 3442–3443. https://doi.org/10.1021/acs.est.0c07856.
Kinahan, A., Hosoda, M., Kelleher, K., Tsujiguchi, T., Akata, N., Tokonami, S., León Vintró, L., 2020. Assessment of radiation dose from the consumption of bottled drinking water in Japan. Int. J. Environ. Res. Publ. Health 17 (14), 4992. https://doi.org/10.3390/ijerph17144992.
Kovács-Bodor, P., Csondor, K., Erőss, A., Szieberth, D., Freiler-Nagy, Á., Horváth, Á., Bihari, Á., Mádl-Szőnyi, J., 2019. Natural radioactivity of thermal springs and related precipitates in Gellért Hill. J. Environ. Radioact. 201, 32–42. https://doi.org/10.1016/j.jenvrad.2019.01.020.
Ma, R., Zheng, C., Prommer, H., Greskowiak, J., Liu, C., Zachara, J., Rockhold, M., 2010. A field-scale reactive transport model for U (VI) migration influenced by coupled multirate mass transfer and surface complexation reactions. Water Resour. Res. 46 (5) https://doi.org/10.1029/2009WR008168.
Ma, R., Zheng, C., Liu, C., Greskowiak, J., Prommer, H., Zachara, J.M., 2014. Assessment of controlling processes for field-scale uranium reactive transport under highly

transient flow conditions. Water Resour. Res. 50 (2), 1006–1024. https://doi.org/10.1002/2013WR013835.
Magyar, I., Sztanó, O., Sebe, K., Katona, L., Csoma, V., Görög, Á., Tóth, E., Szuromi-Korecz, A., Šujan, M., Braucher, R., Ruszkiczay-Rüdiger, Z., Koroknai, B., Wórum, G., Sant, K., Kelder, N., Krigjsman, W., 2019. Towards a high-resolution chronostratigraphy and geochronology for the pannonian stage: significance of the paks cores (central pannonian basin). Foldtani Kozlony 149, 351–369. https://doi.org/10.23928/foldt.kozl.2019.149.4.351.
Mádl-Szőnyi, J., Tóth, J., 2009. A hydrogeological type section for the Duna-Tisza Interfluve, Hungary. Hydrogeol. J. 17 (4), 961–980. https://doi.org/10.1007/s10040-008-0421-z.
Mahoney, J.J., Cadle, S.A., Jakubowski, R.T., 2009. Uranyl adsorption onto hydrous ferric oxide - a re-evaluation for the diffuse layer model database. Environ. Sci. Technol. 43 (24), 9260–9266. https://doi.org/10.1021/es901586w.
Maia, F.M., Ribet, S., Bailly, C., Grivé, M., Madé, B., Montavon, G., 2021. Evaluation of thermodynamic data for aqueous Ca-U (VI)-CO3 species under conditions characteristic of geological clay formation. Appl. Geochem. 124, 104844 https://doi.org/10.1016/j.apgeochem.2020.104844.
Mezősi, G., 2015. Granite weathering in velence hills. In: Lóczy, D. (Ed.), Landscapes and Landforms of Hungary. Springer International Publishing, Switzerland, pp. 89–95. https://doi.org/10.1007/978-3-319-08997-3, 2015.
Minda, M., Tóth, G., Horváth, I., Barnet, I., Hámori, K., Tóth, E., 2009. Indoor radon mapping and its relation to geology in Hungary. Environ. Geol. 57 (3), 601–609. https://doi.org/10.1007/s00254-008-1329-6.
Moog, H.C., Bok, F., Marquardt, C.M., Brendler, V., 2015. Disposal of nuclear waste in host rock formations featuring high-saline solutions–Implementation of a thermodynamic reference database (THEREDA). Appl. Geochem. 55, 72–84. https://doi.org/10.1016/j.apgeochem.2014.12.016.
Mühr-Ebert, E.L., Wagner, F., Walther, C., 2019. Speciation of uranium: compilation of a thermodynamic database and its experimental evaluation using different analytical techniques. Appl. Geochem. 100, 213–222. https://doi.org/10.1016/j.apgeochem.2018.10.006.
Muniruzzaman, M., Haberer, C.M., Grathwohl, P., Rolle, M., 2014. Multicomponent ionic dispersion during transport of electrolytes in heterogeneous porous media: experiments and model-based interpretation. Geochem. Cosmochim. Acta 141, 656–669. https://doi.org/10.1016/j.gca.2014.06.020.
Muniruzzaman, M., Rolle, M., 2015. Impact of multicomponent ionic transport on pH fronts propagation in saturated porous media. Water Resour. Res. 51, 6739–6755. https://doi.org/10.1002/2015WR017134.
Muniruzzaman, M., Rolle, M., 2017. Experimental investigation of the impact of compound-specific dispersion and electrostatic interactions on transient transport and solute breakthrough. Water Resour. Res. 53, 1189–1209. https://doi.org/10.1002/2016WR019727.
Muniruzzaman, M., Rolle, M., 2019. Multicomponent ionic transport modeling in physically and electrostatically heterogeneous porous media with PhreeqcRM coupling for geochemical reactions. Water Resour. Res. 55, 11121–11143. https://doi.org/10.1029/2019WR026373.
Osmond, J.K., Cowart, J.B., Ivanovich, M., 1983. Uranium isotopic disequilibrium in ground water as an indicator of anomalies. Int. J. Appl. Radiat. Isot. 34 (1), 283–308. https://doi.org/10.1016/0020-708X(83)90132-1.
Parkhurst, D.L., Appelo, C.A.J., 2013. Description of Input and Examples for PHREEQC Version 3: a Computer Program for Speciation, Batch-Reaction, One-Dimensional Transport, and Inverse Geochemical Calculations (No. 6-A43). US Geological Survey. https://doi.org/10.3133/tm6A43.
Pérez-Moreno, S.M., Guerrero, J.L., Mosqueda, F., Gázquez, M.J., Bolívar, J.P., 2020. Hydrochemical behaviour of long-lived natural radionuclides in Spanish groundwaters. Catena 191, 104558. https://doi.org/10.1016/j.catena.2020.104558.
Porcelli, D., Swarzenski, P.W., 2003. The behavior of U- and Th-series nuclides in groundwater. Rev. Mineral. Geochem. 52 (1), 317–361. https://doi.org/10.2113/0520317.
Rama, Moore, W.S., 1984. Mechanism of transport of U-Th series radioisotopes from solids into groundwater. Geochem. Cosmochim. Acta 48 (2), 395–399. https://doi.org/10.1016/0016-7037(84)90261-8.
Rolle, M., Muniruzzaman, M., Haberer, C.M., Grathwohl, P., 2013. Coulombic effects in advection-dominated transport of electrolytes in porous media: multicomponent ionic dispersion. Geochem. Cosmochim. Acta 120, 195–205. https://doi.org/10.1016/j.gca.2013.06.031.
Sheppard, M.I., 1980. The Environmental Behavior of Uranium and Thorium (Technical Report AECL-6795). Whiteshell Nuclear Research Establishment. Atomic Energy of Canada Limited, Pinawa, Manitoba, p. 44, 0067-0367.
Sherif, M.I., Sturchio, N.C., 2018. Radionuclide geochemistry of groundwater in the eastern desert, Egypt. Appl. Geochem. 93, 69–80.
Soler, J.M., Steefel, C.I., Gimmi, T., Leupin, O.X., Cloet, V., 2019. Modeling the ionic strength effect on diffusion in clay. The DR-A experiment at Mont Terri. ACS Earth Space Chem 3, 442–451. https://doi.org/10.1021/acsearthspacechem.8b00192.
Stackelberg, P.E., Szabo, Z., Jurgens, B.C., 2018. Radium mobility and the age of groundwater in public-drinking-water supplies from the Cambrian-Ordovician aquifer system, north-central USA. Appl. Geochem. 89, 34–48. https://doi.org/10.1016/j.apgeochem.2017.11.002.
Steefel, C.I., Appelo, C.A.J., Arora, B., Jacques, D., Kalbacher, T., Kolditz, O., et al., 2015. Reactive transport codes for subsurface environmental simulation. Comput. Geosci. 19, 1–34. https://doi.org/10.1007/s10596-014-9443-x.
Surbeck, H., 1996. A radon-in-water monitor based on fast gas transfer membranes. In: International Conference on Technologically Enhanced Natural Radioactivity Caused by Non-uranium Mining, Szczyrk, Poland.
Surbeck, H., 2000. Alpha spectrometry sample preparation using selectively adsorbing thin films. Appl. Radiat. Isot. 53 (1–2), 97–100. https://doi.org/10.1016/S0969-8043(00)00119-6.
Swarzenski, P.W., 2007. U/Th series radionuclides as coastal groundwater tracers. Chem. Rev. 107 (2), 663–674. https://doi.org/10.1021/cr0503761.
Szabo, Z., Vincent, T., Fischer, J.M., Kraemer, T.F., Jacobsen, E., 2012. Occurrence and geochemistry of radium in water from principal drinking-water aquifer systems of the United States. Appl. Geochem. 27 (3), 729–752. https://doi.org/10.1016/j.apgeochem.2011.11.002.
Szilágyi, Á., Glöckner, J.-né, 1971. Jelentés a Balatonfő És Velencei-Hegység D-I Előterében a Pannóniai Képződményekben Végzett Hasadóanyag Kutatásról, 1970. Kézirat. A Mecsekérc Rt. Adattára, Pécs.
Sztanó, O., Magyar, I., Szónoky, M., Lantos, M., Müller, P., Lenkey, L., Katona, L., Csillag, G., 2013. A Tihanyi Formáció a Balaton környékén: Típusszelvény, képződési körülmények, rétegtani jellemzés. Foldtani Kozlony 143 (1), 73–98.
Sztanó, O., Kováč, M., Magyar, I., Šujan, M., Fodor, L., Uhrin, A., Rybár, S., Csillag, G., Tőkés, L., 2016. Late Miocene sedimentary record of the Danube/Kisalföld Basin: interregional correlation of depositional systems, stratigraphy and structural evolution. Geol. Carpathica 67 (6), 525–542. https://doi.org/10.1515/geoca-2016-0033.
Thamó-Bozsó, E., 2002. Magyarországi kainozoos homokok és homokkövek ásványi alkotói és származásuk meghatározásának lehetősége. In: Magyar Állami Földtani Intézet Éves Jelentése 1997–1998-ról. Budapest, pp. 119–134.
Torres, S.B., Petrik, A., Szabó, K.Z., Jordan, G., Yao, J., Szabó, C., 2018. Spatial relationship between the field-measured ambient gamma dose equivalent rate and geological conditions in a granitic area, Velence Hills, Hungary: an application of digital spatial analysis methods. J. Environ. Radioact. 192, 267–278. https://doi.org/10.1016/j.jenvrad.2018.07.00.
Tóth, J., 1999. Groundwater as a geologic agent: an overview of the causes, processes, and manifestations. Hydrogeol. J. 7 (1), 1–14. https://doi.org/10.1007/s100400050176.
Tóth, J., 2009. Gravitational Systems of Groundwater Flow: Theory, Evaluation, Utilization. Cambridge University Press, Cambridge, UK, p. 297.
Tournassat, C., Steefel, C.I., 2015. Ionic transport in nano-porous clays with consideration of electrostatic effects. Rev. Mineral. Geochem. 80, 287–329. https://doi.org/10.2138/rmg.2015.80.09.
Vesterbacka, P., Turtiainen, T., Heinävaara, S., Arvela, H., 2006. Activity concentrations of 226Ra and 228Ra in drilled well water in Finland. Radiat. prot. dosim. 121 (4), 406–412. https://doi.org/10.1093/rpd/ncl067.
Vinogradov, A.P., 1962. Average contents of chemical elements in the principal types of igneous rocks of the earth's crust. Geochemistry 7, 641–664.
Wolkersdorfer, C., 2008. Water Management at Abandoned Flooded Underground Mines: Fundamentals, Tracer Tests, Modelling, Water Treatment. Springer Science & Business Media, p. 465. https://doi.org/10.1007/978-3-540-77331-3.